Artigo

POSTSYNTHESIS OF TITANIUM INCORPORATED WITH AMINO-FUNCTIONALIZATION UIO-66 FOR ENHANCING CO$_2$ UPTAKE

Jinlong Ge[a,*], **Zhong Wu[a], Qiuqin Wang[a] and Shanshan Yang[a]**
[a]School of Material and Chemistry Engineering, Bengbu University, Bengbu 233030, P. R.China

Metal-organic frameworks (MOFs) are promising nanomaterials with unprecedented capacity to store small molecules. Titanium cooperated with NH$_2$-UiO-66 were prepared via post synthesis modifications approach and their structures and properties were characterized by X-raydiffraction,Fourier transform infrared spectroscopy, thermogravimetric analysis, nitrogen adsorption isotherms, and scanning electron microscopy. The resultant titanium cooperated with NH$_2$-UiO-66 showed excellent performance for CO$_2$ adsorption via the formation of oxo-bridged hetero-Zr–Ti clusters. This result clearly demonstrates that the smaller Ti ions exchanged with the Zr ions of NH$_2$-UiO-66 may decrease the pore sizes within the framework to be closer to the ideal pore sizes for CO$_2$ adsorption.

Keywords: metal-organic frameworks; NH$_2$-UiO-66; CO$_2$ uptake;Titanium

INTRODUCTION

As a new class of hybrid porous crystalline materials, metal-organic frameworks (MOFs) typically constructed from metal oxo-clusters interconnected by polydentate organic ligands, have a definite composition and structure.[1] Permanent microporosity, adjustable porosities, tunable pore suface,typically very high internal surface areas and low densities make MOFs material promising candidates in the area of gas storage,[2] separation, heterogeneous catalysis, chemical sensing and drug delivery. [3] Additionally,porous MOF compounds provide distinct advantages over other classes of adsorbents and heterogeneous catalysts.[4]

Nowadays, the rising level of carbon dioxide in the atmosphere has become one of the biggest problems worldwide.[5] Therefore, reducing carbon dioxide emission from the burning processes by capture and storage has been proposed as one of the control strategies and thus has been studied by many researchers throughout the world using different technologies.[6] With current technology, the most effective method of CO$_2$ capture from flue gases is chemical absorption in an aqueous solution of an amine based organic, such as mono- or diethanol-amine.[7] Furthermore, the degradation of the amine absorbent leads to corrosive mixtures.Among these methods, recent advances have shifted towards adsorption technology using novel materials such as MOFs to controlling the CO$_2$ emission from flue gases.[8] In addition to a high surface area and pore volume, MOFs chemical nature can be fine-tuned by selecting the appropriate building blocks and/or by post-synthetic modification, thus leading to tailored porous materials with great promise for the CO$_2$ adsorption.[9]

Recently, Zr-based MOFs (UiO-66) , which with free diameter of octahedral cage is 11 Å and tetrahedral cage is 8Å, and the cages are connected by triangular windows with a diameter of 6 Å, have been found to have good thermal stability and adsorption capacity toward CO$_2$. Different ligand linkers have been tested for adsorption of CO$_2$ such as NH$_2$-BDC and Br-BDC.[10] Possess high surface areas, large cavity volumes, robust and stable at high temperatures and in atmospheric moisture, NH$_2$-UiO-66 is an ideal candidate for CO$_2$ capture.[11]

The partial substitution of metal cations in MOFs can lead to the formation of oxo-bridged heterometallic assemblies within the same

MOFs. Such bimetallic assemblies with more flexibility and tunability due to the availability of different MOF structures, are expected to show enhanced photocatalytic performance.[12]The incorporation with metal ions in MOFs is considered one of the effective ways to modify the pore sizes of MOFs. Post-synthesis modifications of preconstructed MOFs by replacement of the organic cation with smaller inorganic cation have been performed to tune the pore size and provide desired surface chemistries in MOFs.This postsynthetic exchange of ligands occurred with full retention of crystallinity and porosity as gas sorption measurements.[13]

NH$_2$-UiO-66 is suitable for postsynthetic modification with a variety of anhydrides to generate new functionalized frameworks. The amine tagged NH$_2$-UiO-66 has been explored in post-synthesis modifications reactions, Cohen and Lillerud[14] independently reported the acylation of NH$_2$-UiO-66 via the use of anhydride reagents.The aziridination of the amino group has been performed in NH$_2$-UiO-66 with acetaldehyde. Wang *et al*.[15] reported via a facial modified post-grafting method prepared UiO-66 fabricated with titanium. Ti-substituted NH$_2$ -UiO-66(Zr/Ti) prepared by Sun et.al. using a post-synthetic exchange method showed enhanced photocatalytic performance for both CO$_2$ reduction.

We herein report the synthesis of titanium cooperated with NH$_2$-UiO-66 via a facial modfied post-grafing method. The CO$_2$ adsorption performance of the as-synthesized NH$_2$-UiO-66(Ti) nanocomposites was evaluated.

EXPERIMENTAL

Materials

Zirconium chloride (ZrCl$_4$), 2-aminoterephthalic acid (Sigma-Aldrich.>99%), N,N-dimethylformamide (DMF) and ethanol were purchased from Shanghai Chemical Reaent Inc. of the Chinese Medicine Group. Tetrabutyl titanate(Ti(OBu)$_4$) were ordered from Aladdin,All chemicals were used without further purification.

Synthesis of amino-functionalized NH$_2$-UiO-66

A standard up scaled synthesis of NH$_2$-UiO-66was performed by dissolving ZrCl$_4$(1.50g,6.4mmol) and 2-aminoterephthalic acid (1.56

g, 6.4 mmol) in DMF (180 mL) at room temperature in a volumetric flask.[16] The resulting mixture was placed in a preheated oven at 80 for 12 h and then held at 100 °C for 24 h. After the solution was cooled to room temperature in air, the resulting solid was filtered and repeatedly washed with absolute ethanol for 3 days while heated at 60 °C in a water bath. The resulting yellow powder was filtered and dried under vacuum at ambient temperature.

Synthesis of TiCl$_4$(THF)$_2$

TiCl$_4$(THF)$_2$ was synthesized according to the patent of Francesco *et al.*[17] 5.0 g TiCl$_4$ was dissolved in 50 mL of dichloroethane in a 250mL RBF under inert conditions. 7.62 g dried tetrahydrofuran (THF) was added at 0 °C to form a yellow solution. 100 mL of sodium dried n-hexane was used to precipitate a yellow powder, which was filtered and washed with n-hexane. It was dried for 2-3 hours over a Schlenk line, and used immediately for post-synthetic exchange.

Post-synthetic exchange of UiO-66 with TiCl$_4$ (THF)$_2$

The post-synthetic exchange of UiO-66 with TiCl$_4$(THF)$_2$ was carried out according to the work of Cohen and co-workers. 0.17 g TiCl$_4$ (THF)$_2$ was dissolved in 10 mL of DMF. 0.14 g of NH$_2$-UiO-66 was added. (denoted as NH$_2$-UiO-66 (Ti)-0.2, 0.4, 0.6, 0.8, 1.0, respectively). The mixture was incubated for 5 and 15 days. The solids were separated from the solvent via centrifugation, and washed with fresh DMF. The washed solids were immersed in a methanol bath for 3 days. The methanol was replaced every 24 hours. The solids were dried at 40 °C in a vacuum for 24 hours.

Characterizations

Powder X-ray diffraction (PXRD) patterns were collected by using an X-ray diffract meter with Cu target (36 kV, 25 mA) from 5 to 70°. Ultraviolet-visible (UV-vis) absorbance spectra were collected on a Shimadzu UV 3600 plus spectrophotometer over a range of 200–800 nm. Infrared (IR) spectra (KBr pellets) were obtained in the 400-4000 cm^{-1} rang with a resolution of 4 cm^{-1} using a Nicolet Nexus 870 FTIR spectrometer. Nitrogen sorption-desorption isotherms were obtained at 77 K on a Micromeritics ASAP 3020 analyzer. The samples were heated at 150 °C for 12 h prior to each test. Morphology and microstructure were observed by a field emissions scanning electron microscope (FE-SEM: Hitachi S-4800) and high resolution transmission electron microscopy (TEM: JEOL JEM 2100). Transmission electron microscope was operated at 200kV. Thermogravimetric Analysis was performed on an in the tempteature range of 30-900 °C under nitrogen at a heating rate of 20°C min^{-1},using a Pyris1 TGA-1.

RESULTS AND DISCUSSION

Characterization of Ti/NH$_2$-UiO-66

XRD,FI-IR measurements

XRD patterns of the NH$_2$-UiO-66 and UiO-66(Ti) nanocomposite was presents as Figure 1. All the NH$_2$-UiO-66(Ti) exhibited a similar XRD pattern as reported in the literature. The samples present sharper and narrower diffraction peaks at 2θ=7.3°, 8.5°, 17.1°, 25.8° and 30.8°, indicating the higher crystallinity.[18] Peaks corresponding to newly emerged phases cannot be observed even at higher Ti concentration. It suggested that the introduction of titanium does not result in any destruction or disorder in comparison to the NH$_2$-UiO-66 sample.[19] Additionally, with the increasing of the Ti to Zr molar ratio,

the partial substitution of larger Zr in Zr-O oxoclusters replaced by smaller Ti, this suggests that Zr in the original NH$_2$-UiO-66 has been substituted by Ti.NH$_2$-UiO-66 framework was reformed and substituted by the titanium species with Ti-O clusters,NH$_2$-UiO-66 shows not well-ordered porous structure.[20]
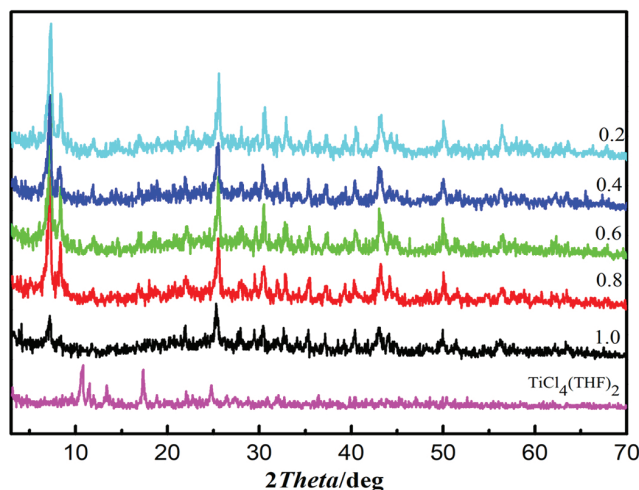
Figure 1.XRD *spectra of Ti incorporated with NH$_2$-UiO-66*

The FTIR spectra of these Ti/NH$_2$-UiO-66 samples exhibit similar characteristic peaks, as shown in Figure 2.The two intense bands around 1569.15 and 1386.53 cm^{-1} are associated with the C-O asymmetric and symmetric stretch vibrations in the carboxylate group in NH$_2$BDC, respectively.[21] The small band around 1497.35cm^{-1} represents the vibration of C-C in the benzene ring. The 1361.25 cm^{-1} absorption band is attributed to the C-N stretching. Additional peaks between 664.89-964.80 cm^{-1} are associated with bending and twisting of the Zr node.[22] Shoulder peaks are associated with the loss of symmetry at the Zr node, but are difficult to distinguish. The Zr-Cl stretch is difficult to assign to one specific mode but occurs in the same frequency range as the Zr-O stretches between 483.20 and 582.96 cm^{-1}.
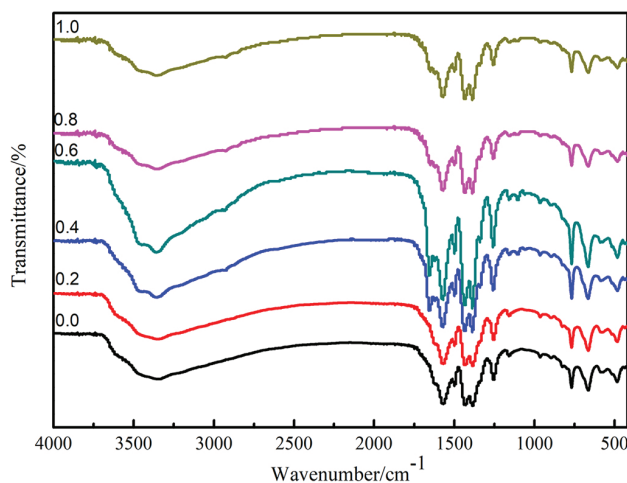
Figure 2.FTIR *spectra of Ti incorporated with NH$_2$-UiO-66*

TG,BET measurements

Thermogravimetric analyses were carried out in an air atmosphere for investigation of the thermal stability of the compound. As displayed in Figure 3, the Ti incorporated with NH$_2$-UiO-66 was accordance with previous studies.[23] The framework decomposition is occurs

over a temperature range of 540 °C. All the samples are occur loss of physisorbed water molecules and solvent molecules hosted in the pores over a temperature range of 35-100 °C. The progressive structured weight loss up to 200-350 °C are the removal of monocarboxylate ligands and dehydroxylation of the Zr 6 cornerstones.[24] However, increasing the Ti concentration in the post-synthetic metal results in the plateau increasing toward ideality, indicating that more Ti have been exchange in NH_2-UiO-66 structure. The TGA plateau is in fact found to systematically increase with the ratio of Ti to Zr.[25]
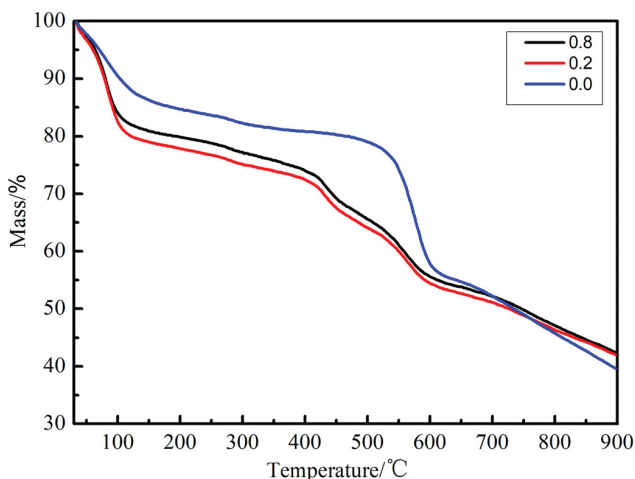
Figure 3.TG *spectra of Ti incorporated with NH_2-UiO-66*

The N_2 adsorption–desorption isotherm measurement and the pore-size was performed distribution curve are shown in Figure 4. We can see that the nitrogen adsorption capacity varies significantly depending on content of Ti.

The specific BET surface area of 1227 m^2 g^{-1} of NH_2-UiO-66 and varied to 627,563,509,484,350 m^2 g^{-1} with increasing of the Ti concentration, respectively.

NH_2-UiO-66(Ti) presents the lowest BET of 350 m^2 g^{-1}. The decreased BET indicates that the pores in the NH_2-UiO-66 nanocomposites are smaller than the parent NH_2-UiO-66.[26] Such phenomena are frequently observed over inorganic semiconductor solid solutions and suggest the substitution of larger Zr^{4+} in Zr-O oxo-clusters by smaller Ti^{4+}, which results in the shrinking of the crystal lattice in the porous material.[27]
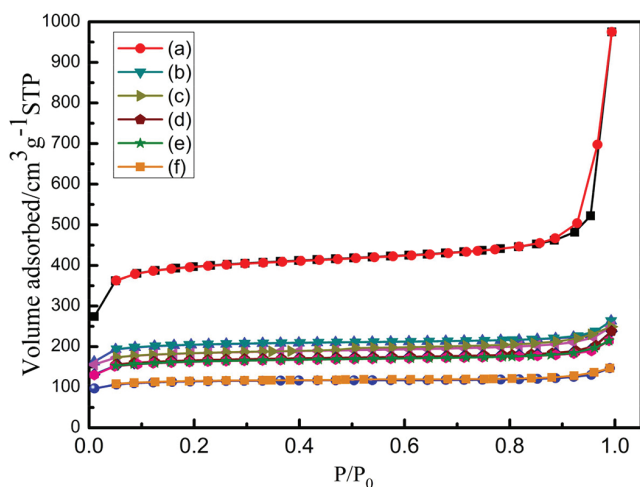
Figure 4. *N_2 adsorptiondesorption isotherms of Ti incorporated with NH_2-UiO-66*

Table1. BET and pore volume of the different Ti incorporated with NH_2-UiO-66

Ti/Zr	BET (m^2 g^{-1})	Langmuir (m^2 g^{-1})	pore vol (cm^3 g^{-1})
0	1227.6	1889.4	0.52
0.2	627.0	935.2	0.46
0.4	563.4	855.4	0.48
0.6	509.6	773.9	0.42
0.8	484.2	755.5	0.38
1.0	350.0	515.9	0.30

UV-vis measurements

The UV-visible absorption spectra are presented in Figure 5. It shows that two main absorption peaks at around 265 and 365 nm. The peak at 265 nm is ascribed to the absorption of Zr-O clusters in the NH_2-UiO-66. The peak is broader than the unsubstituted NH_2-UiO-66, this result may be attributed to the absorption of Ti-O oxo-clusters generated by Ti substitution in NH_2-UiO-66.[28] The main peak at 365 nm is ascribed to the ligand based absorption influenced by the nearby metal centers. However, these two peaks become broader and more intense after the titanium was incorporated into NH_2-UiO-66.[29] In addition, the UV-vis absorption edges of the as-prepared NH_2-UiO-66(Ti) nanocomposites are shifted to longer wavelengths compared with that of NH_2-UiO-66. The absorption bands in the near visible and visible regions in NH_2-UiO-66(Ti) are mainly attributed to the ligand to metal charge transfer and can be assigned to the interaction between the ligand and substituted Ti.[30]
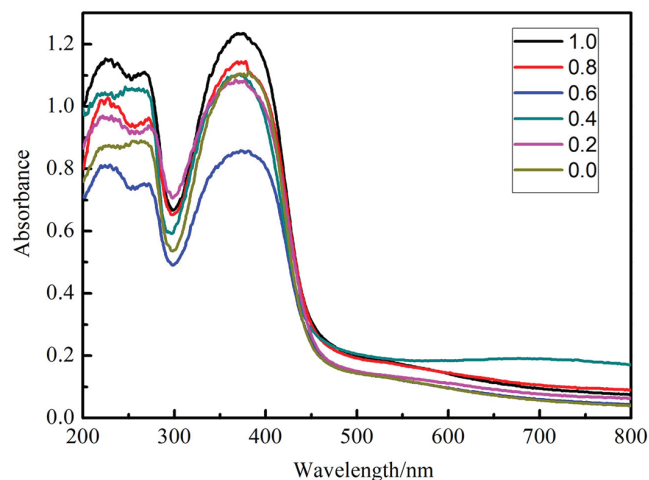
Figure 5. *UV-vis spectra of Ti incorporated with NH_2-UiO-66*

XPS measurements

The X-ray photoelectron spectroscopy (XPS) is a highly sensitive technique to explore the chemical changes in the element surroundings. The XPS spectra of the elements of interest Zr3d, Ti2p, N1s, O1s are shown in Figure 6.The survey scan of the NH_2-UiO-66 and NH_2-UiO-66(Ti) was shown in Figure 6(a), new peaks associated with Ti2p appeared in the XPS spectrum of the UiO-66(Ti) composites, and their relative peak intensities to that of Zr3p increased with an increasing Ti content. These observations confirmed that the titanium moieties were successfully.The analysis Figure 6(c) of NH_2-UiO-66(Ti) indicated a small shift in the binding energy of the Zr3d peaks (from 185.08 and 182.78 eV to 185.28 and 182.88eV,respectively).[31] Figure 6(d) shows two peaks of the Ti2p region at 458.7 eV and 464.5 eV,corresponding to Ti2p3/2 and Ti2p1/2
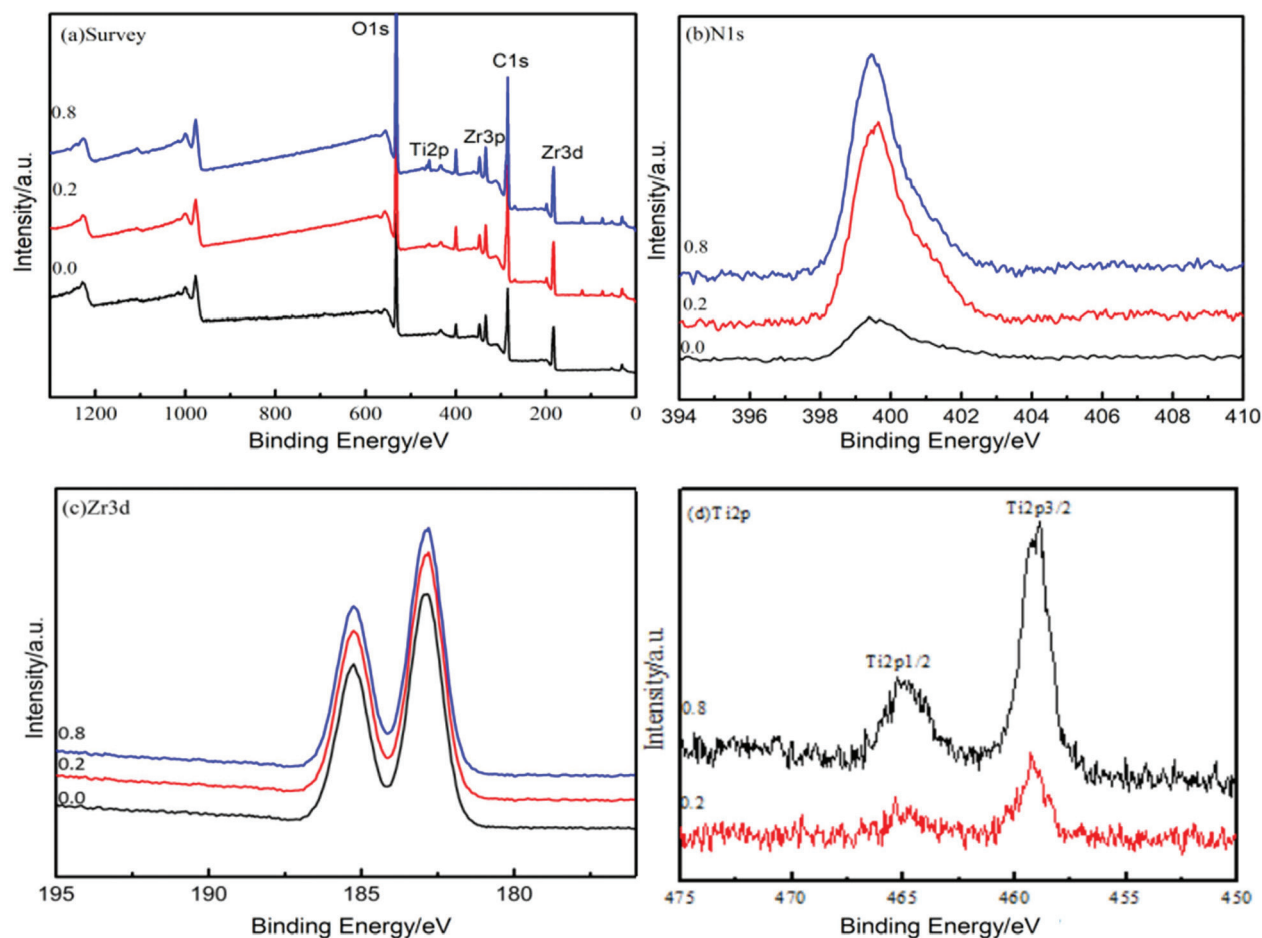
Figure 6. *XPS spectra of Ti incorporated with NH₂-UiO-66*

respectively, The increasing Ti contents could be explained by the enhanced electron density around the O atoms. All these features imply that the titanium moieties be introduced to the framework of UiO-66 as electron donor via the formation of oxo-bridged hetero-Zr–Ti clusters.and provided that another confirmation of the successful incorporation of the Ti moiety in NH_2-UiO-66.[32]

SEM and TEM measurements

The morphology of NH_2-UiO-66 and the NH_2-UiO-66(Ti) nanocomposite were investigated by SEM. According to Figure 7, it can be clearly seen from (a) that NH_2-UiO-66 nanocrystals were more angular, revealing the increased definition of facets and vertices that are common in larger crystals, indicating that the presence of the NH_2 group on the organic linker affects the growth mechanism of the framework.[33] The materials have the typical octahedral morphology, with homogeneous particle diameters about 200 nm. Obviously, NH_2-UiO-66(Ti) retained the similar morphology as NH_2-UiO-66. Furthermore, no obvious differences of the morphologies could be observed from the TEM images (g and h). These observations suggest that Ti was truly incorporated into the UiO-66 framework to replace Zr as skeleton.[34] No change in the octahedral morphology of the crystals could be observed. Furthermore, EDS elemental analysis was also conducted to study the elemental distribution. The EDS spectrum of NH_2-UiO-66(Ti) reveals N, Zr, Ti, and O elements.

CO₂ adsorption

The CO_2 adsorption isotherms for NH_2-UiO-66(Ti) are shown in Figure 8. All MOFs exhibited a type I isotherm, which is indeed characteristic of microporous materials. NH_2-UiO-66(Ti)-0.2 and NH_2-UiO-66(Ti)-0.4 samples presented higher CO_2 adsorption than NH_2-UiO-66 sample. And the two samples show the highest CO_2 adsorption capacities.NH_2-UiO-66(Ti)-0.6 has the similar adsorption capacity as NH_2-UiO-66. The rate of 0.8 and 1.0 are lower than NH_2-UiO-66. Considering the moderate BET surface area and pore volume of Titanium incorporated with NH_2-UiO-66, it is likely that the high CO_2 capacity is due to the average pore diameter being of an optimal size to confine CO_2 molecules.[35] This suggests that Zr in the original NH_2-UiO-66 has been substituted by Ti. The Ti-O ring sterically hinders access to the stronger adsorption sites at the metal cluster.[36] It is noted that Ti has produced a higher affinity for adsorption of CO_2.[37] Ti incorporated with NH_2 functional groups can provide more CO_2 adsorption sites and increase the affinity toward CO_2.Several studies have been reported that the presence of micropores (<0.8 nm) in porous carbons showed superior CO_2 adsorption capacity, particularly for CO2 capture at atmospheric pressure and room temperature. The results of CO_2 adsorption indicate that not only the amount of defects but also their charge compensating groups within the materials have a marked effect on the loading of guest molecules.[38,39] An important observation is the amount of uptake that occurs within the small cavities. This is remarkable considering that the small cavities of ~5 Å appear to have a large role in the uptake of CO_2.The Titanium cooperated with NH_2-UiO-66 herein illustrate the importance of reactive side groups, introduced in post-synthetic modifications, converted in high yields to functionalities through post-synthetic methods.[40] Moreover, our work highlights the strategies of tailoring host-guest
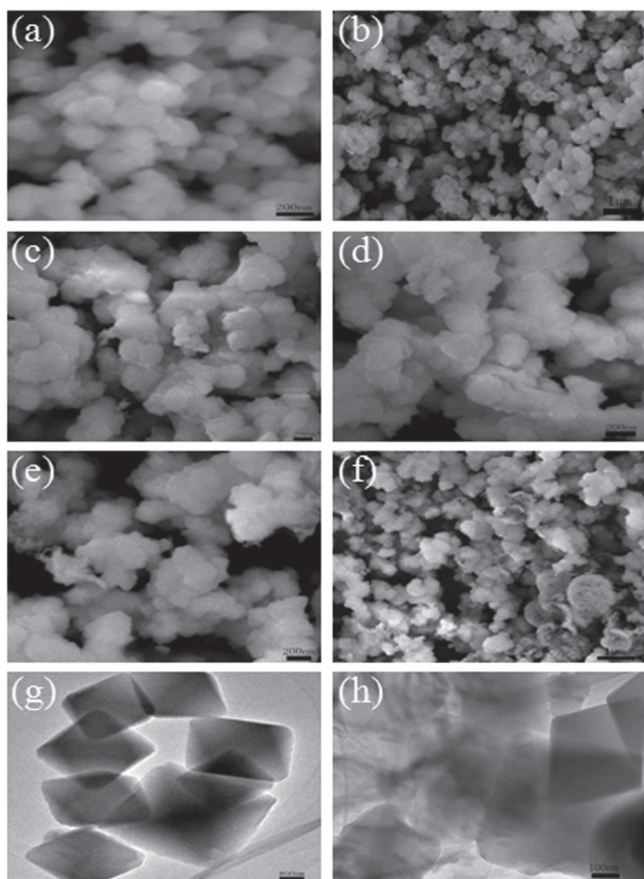
Figure 7 . SEM and TEM spectra of representative Ti incorporated with NH$_2$-UiO-66
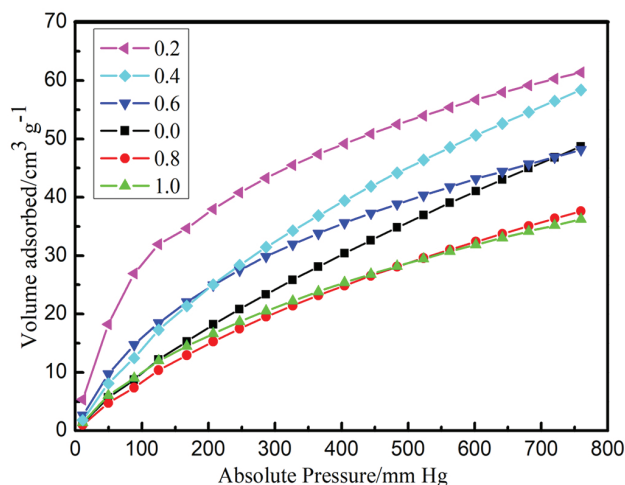
Figure 8. CO_2 adsorption isotherms of Ti incorporated with NH$_2$-UiO-66

interactions through post-synthetic method, therefore, enabling applications in CO_2 uptake.

Metal organic framework NH$_2$-UiO-66 fabricated with titanium was successfully prepared via a facial modified post synthesis method. Zr ions in NH$_2$-UiO-66 were post synthetically exchanged with Ti ions at different loading rate. The Ti-exchanged NH$_2$-UiO-66 enhanced CO_2 adsorption could be attributed to the the substituted Ti center. This result clearly demonstrates that the Ti ions may decrease the pore sizes within the framework to be closer to the ideal pore sizes for CO_2 adsorption,which are critical to the enhancing of the CO_2 adsorption.

REFERENCES

1. Huang, Y. H.; Lo, W. S.; Kuo, Y. W.; Chen, W J.; Lin, C. H.; Shieh, F. K.; *Chem. Commun.* **2017**, *43*, 5818.

2. Zhou, H. F; Liu, B.; Hou, L.; Zhang, W. Y.; Wang, Y. Y.; *Chem. Commun*. **2018**, *54,* 456.

3. Zhu, S. Y.; Yan, B.; *Dalton Trans*. **2018**, *47*, 1674.

4. Hu, Z.; Zhao, D.; *Dalton Trans*. **2015**, *44*, 19018.

5. Han, Y. T; Liu, M.; Li, K. Y; Sun, Q.; Zhang, W. S.; Song, C. S.; Zhang, G. L.; Zhang, Z. C.; Guo, W; *Inorg. Chem. Front*. **2017**, *4*, 1870.

6. Yang, J.; Zhang, F. J; Wang, X.; He, D. S.; Wu, G.; Yang, Q. H.; Hong, X.; Wu, Y.; Li, Y. D.; *Angew. Chem. Int. Ed*. **2016**, *55*, 12854.

7. Yao, B. J.; Jiang, W. L.; Dong, Y.; Liu, Z. X.; Dong, Y. B.; *Chem. Eur. J.* **2016**, *22*, 10565.

8. Zhong, Z. W; Pang, S. L.; Wu, Y. W.; Jiang, S.; Ouyang, J.; *J .Chem. Technol. Biotechnol*. **2017**, *92*, 1841.

9. Liu, J. L.; Zhu, D. D.; Guo, C. X.; Vasileff, A.; Qiao, S. Z.; *Adv. Energy. Mater* **2017**, 1700518.

10. Taddei, M.; Dau, P. V.; Cohen, S. M.; Ranocchiari, M.; Bokhoven, J.; Costantino, F.; Sabatino, S.; Vivani, R.; *Dalton. Trans*. **2015**, *44*, 14019.

11. Zou, G. Z.; Hou, H. S.; Zhao, G. G.; Ge, P.; Yin, D. L.; Ji, X. B. *J. Mater. Chem. A* **2015**, *6*, 4839.

12. Ragon, F.; Chevreau, H.; Devic, T.; Serre, C.; Horcajada, P.; *Chem. Eur. J.* **2015**, *21*, 7135.

13. Wu, M. X.; Yang, Y. W.; *Adv. Mater* **2017,** *29*, 1606134.

14. Zhang, X. P; Sun, W. D; Du, H. T; Kong, R. M.; Qu, F. L.; *Inorg. Chem. Front*. **2018**, 5344.

15. Wang, A. N.; Zhou, Y. J.; Wang, Z. L.; Chen, M.; Sun , L. Y.; Liu, X. *RSC. Adv*. **2016**, *6*, 3671.

16. Peng, Y. G.; Huang , H. L.; Zhang, Y. X.; Kang, C. F.; Chen, S. M.; Song, L.; Liu, D. H.; Zhong, C. L.; *Nature Commun*. **2018**, *9*, 187.

17. Sutrisna, P. D.; Hou, J. W.; Zulkifli, M. Y.; Li, H. Y.; Zhang, Y. T.; Liang, W. B.; DAless, D. M.; Chen, V.; *J. Mater. Chem. A* **2018**, *6*, 918.

18. Han, Y. T.; Liu, M.; Li, K. Y.; Zuo, Y.; Wei, Y. X.; Xu, S. T.; Zhang, G. L.; Song, C. S.; Zhang, Z. C.; Guo, X. W.; *CrystEngComm*. **2015**, *17*, 6434.

19. Hu, Z. G.; Nalaparaju, A.; Peng, Y. W.; Jiang, J. W.; Zhao, D.; *CrystEngComm*. **2015**, *17*, 6434.

20. Sadeghzadeh, S. M.; Zhiani, R.; Emrani, S.; *New. J. Chem*. **2018**, *42*, 988.

21. Anjum, M. W.; Vermoortele, F.; Khan, A. L.; Bueken, B.; DeVos, D.; Vankelecom, I.; *ACS Appl. Mater. Interfaces*. **2015**, *5*, 25193.

22. Xian, S. K.; Wu, Y.; Wu, J. L.; Wang, X.; Xiao, J.; *Ind. Eng. Chem. Res*. **2015**, *54*, 11151.

23. Nguyen, H.; Mao, L.; Peters, A. W.; Audu, C. O.; Brown, Z. J.; Farha, O. K.; Hupp, J. T.; Nguyen, S. T.; *Catal. Sci. Technol*. **2015**, *5*, 4444.

24. Shearer, G. C.; Chavan, S.; Ethiraj, J.; Vitillo, J. G.; Svelle, S.; Olsbye, U.; Lamberti, C.; Bordig, S.; Lillerud, K. P.; *Chem.Mater* **2014**, *26*, 4068.

25. Shearer, G. C.; Chavan, S.; Bordig, S.; Svelle, S.; Olsbye, U.; Lillerud, K. P.; *Chem. Mater*. **2016**, *28*, 3749.

26. Valenzano, L.; Civalleri, B.; Chavan, S.; Bordig, S.; Nilsen, M .H.; Jakobsen, S.; Lillerud, K. P.; Lamberti, C.; *Chem. Mater* **2011**, *23*, 1700.

27. Miao, Z. C.; Qi, C.; Wensley, A. M.; Luan, Y.;*RSC Adv*. **2016**, *6*, 67226.

28. Sun, D. R.; Liu, W. J.; Mei, Q. M.; Zhang, Y. F.; Li, Z. C.; *Commun*. **2015**, *51*, 2056.

29. Ghalei, B.; Sakurai, K.; Kinoshita, Y.; Wakimoto, K.; Isfahani, P.; Song, Q. L.; Doitomi, K.; Furukawa, H.; Hajime, H.; Kitagawa.S.; Sivaniah, E.; *Nature Energy* **2017**, *2,* 17086.

30. Karagiaridi, O.; Vermeulen, N. A.; Klet, R. C.; Wang, T. C.; Moghadam, P. Z.; Farha, O. K.; *Inorg. Chem.* **2015**, *54*, 1785.

31. Buragohain, A.; Biswas, S.; *CrystEngComm.* **2016**, *18*, 4374.

32. Sava, G. F.; Harvey, J.; Pearce, C.; Hall, M.; De Coste, Jared.; Kinnan, M.; Greathouse,J.; *J.Mater.Chem.A* **2018**, *6*, 3038.

33. Yang, J.M.; Ying, R. J; Han, C. X; Hu, Q. T; Xu, H. M.; Li, J. H.; Wang, Q.; Zhang, W.; *Dalton Trans.* **2018**, *47*, 3913.

34. Gao, X. C; Hai, X; Baigude, H.; Guan, W. H.; Liu,Z. L.; *Scientific Reports* **2016**, *6*, 37705.

35. Kaposi, M.; Cokoja, M.; Hutterer ,C. H.; Hauser, S. A.; Kaposi, T.; Klappenberger,F.;Pötg, A.; Barth, J.; Herrmanna, W.; Kühn, F. E.; *Dalton Trans.* **2015**, *44*, 15976.

36. Trickett, C. A.; Gagnon, K. J.; Lee, S.; Felipe, G.; Bîrgi , H. B.; Yaghi, O. M.; *Angew. Chem. Int. Ed.* **2015**, *54*, 11162.

37. Ye, G.; Qi, H.; Li, X. L.; Leng, K. Y.; Sun, Y. Y.; Xu, W.; *ChemPhysChem.* **2017**, *18*, 1903.

38. Gadipelli, S.; Guo, Z. X.; *Chem. Mater* **2014**, *26*, 6333.

39. Gascón,V.; Miguel, E. C.; García, M. D.; Blanco, R. M.; Sanchez, S. M.; *J Chem Technol Biotechnol*. **2017**, *92*, 2583.

40. Kronast, A.; Eckstein, A.; Altenbuchner, P.T.; Hindelang, K.; Vagin, S.; Rieger, B.; *Chem. Eur. J*. **2016**, *22*, 12800.